Supporting Information

Thermoelectric performance of organic conductors

Takehiko Mori

Department of Materials Science and Engineering, Tokyo Institute of Technology, O-okayama 2-12-1, Meguro-ku, Tokyo 152-8552, Japan. E-mail: mori.t@mac.titech.ac.jp

Calculation of thermoelectric power

Eqn (2) is numerically integrated.[47,48]

$$K_0 = \tau \iiint v^2 \left(-\frac{df_0}{dE} \right) dk^3 = \frac{\tau}{\hbar^2} \frac{N_x \sum \Delta E^2 \left(-\frac{df_0}{dE} \right) a\pi}{N_y N_z \quad bc} \tag{S1}$$

The second form for v_x is derived from the following relation.

$$v_x = \frac{1}{\hbar} \frac{\partial E(k)}{\partial k_x} = \frac{N_x a \Delta E}{\pi} \tag{S2}$$

The Brillouin zone is divided by a mesh of $N_x \times N_y \times N_z$, and $E(k)$ is calculated at the respective points. $E(k)$ is estimated from the tight-binding energy band considering only the highest occupied molecular orbital (HOMO) or lowest unoccupied molecular orbital (LUMO).[S1,S2] The interval of k contains $\Delta k_x = \pi/aN_x$, where Δk_x appears not only in the denominator coming from eqn (S2) but also in the numerator from the integration in eqn (S1). Accordingly, N_yN_z appears as the number of the summation, and N_x comes from the segment of the v_x calculation. In the actual calculation, the coefficient of eqn (S1) is $\pi e^3/\hbar^2 = 1.2867 \times 10^{14}$ C^2 Å J^{-1} s^{-2} cm^{-2}, where $(-df_0/dE)$ is proportional to inverse temperature and represented in eV^{-1} unit. Eqn (3) is estimated similarly.

For β-(BEDT-TTF)$_2$I$_3$, κ-(BEDT-TTF)$_2$Cu(NCS)$_2$, and α-(BEDT-TTF)$_2$NH$_4$Hg(SCN)$_4$, transfer integrals that are optimized so as to reproduce the observed thermoelectric power are used.[47,48] The reported transfer integrals are used for other cases.

When the Fermi energy crosses more than two energy bands, K_0 and K_1 are summed for these bands.

$$S = \frac{1}{eT} \frac{\sum_i K_{1i}}{\sum_i K_{0i}} = \frac{1}{eT} \frac{\sum_i (K_{1i}/K_{0i}) K_{0i}}{\sum_i K_{0i}} = \frac{\sum_i S_i \sigma_i}{\sum_i \sigma_i} \tag{S3}$$

Here, K_{0i} represents K_0 for different energy bands i. Using eqn (5), this is a weighted average of S_i with respect to σ_i.

K_0 and K_1 of TTF donors

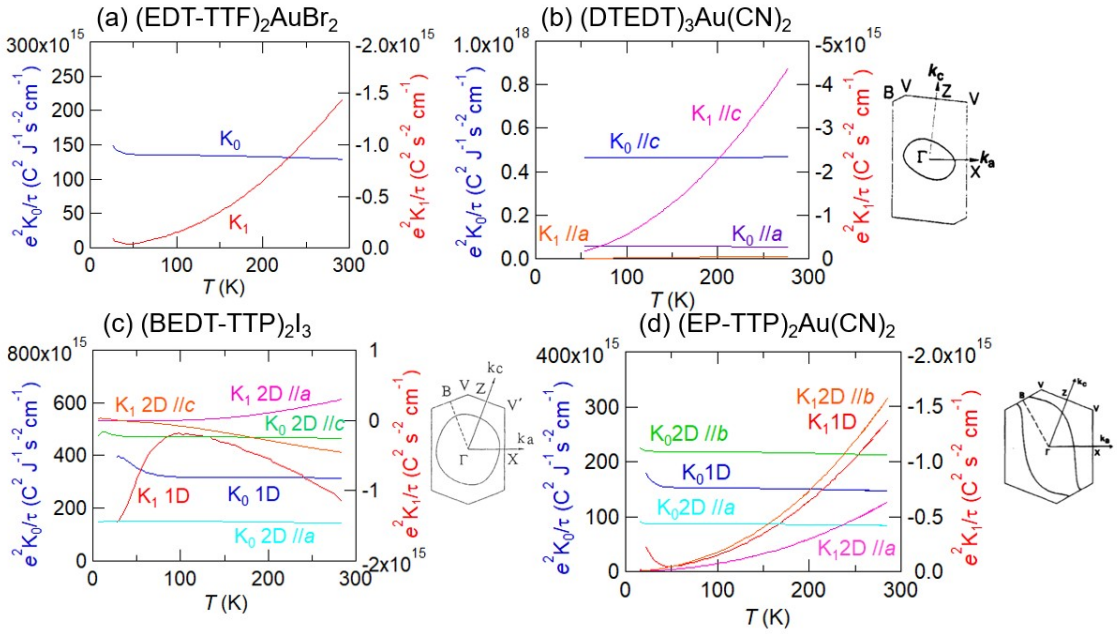

Fig. S1 Calculated K_0 and K_1 integrals, and the Fermi surface of (a) $(EDT\text{-}TTF)_2AuBr_2$, (b) $(DTEDT)_3Au(CN)_2$, (c) $(BEDT\text{-}TTP)_2I_3$, and (d) $(EP\text{-}TTP)_2Au(CN)_2$.

Table S1 Relaxation time (τ) and calculated K_0 and K_1 integrals.

Compound	axis	τ_{rt}	τ_{max}	axis	e^2K_0/τ (rt)	e^2K_1/τ (rt)
		$\times 10^{-15}$ (s)			$\times 10^{15}$ (C^2 J^{-1} s^{-2} cm^{-1})	$\times 10^{15}$ (C^2 s^{-2} cm^{-1})
(TTF)(TCNQ)	stack	7	70	stack	58	0.49
$(TMTSF)_2PF_6$	stack	1.6	600	stack	310	−2.7
β-$(BEDT\text{-}TTF)_2I_3$	*a*	0.3	100	*a*/*b*	120/210	−1.2/−1.5
κ-$(BEDT\text{-}TTF)_2Cu(NCS)_2$	*c*	0.7	130	*c*/*b*	14/8	−0.73/0.62
α-$(BEDT\text{-}TTF)_2KHg(SCN)_4$	*c*	0.1	1.8	*c*/*a*	55/560	−0.2/2.1
α-$(BEDT\text{-}TTF)_2NH_4Hg(SCN)_4$	*c*	1.2	700	*c*/*a*	19/210	−0.17/1.8
α-$(BEDT\text{-}TTF)_2I_3$	*a*	0.3	1.5	*a*/*b*	56/47	−1.6/0.70
θ-$(BEDT\text{-}TTF)_2CsCo(SCN)_4$	*c*	3	7	*c*/*a*	12/82	−0.12/−0.46
β-$(BEDT\text{-}TTF)_2PF_6$	*c*	0.6	0.72	*c*/*a*	14/71	−0.21/0.47
β“-$(BEDT\text{-}TTF)_4Pd(CN)_4H_2O$	*a*	0.4		*a*/*c*	210/400	−0.74/−2.2
$(EDT\text{-}TTF)_2AuBr_2$	stack	1.2	2.6	stack	130	−1.4
$(DTEDT)_3Au(CN)_2$	*c*	3.2	48	*c*/*a*	470/54	−4.4/0.054
$(BEDT\text{-}TTP)_2I_3$	*c*	2.2	75	*c*/*a*	470/140	−0.45/0.30
$(EP\text{-}TTP)_2Au(CN)_2$	stack	7.2	100	*a*/*c*	210/84	−1.6/−0.63
$(TTM\text{-}TTP)(I_3)_{3/5}$	stack	1.8	3.0	stack	140	2.3
$(BTBT)_2AsF_6$	stack	12	43	stack	550	−2.7
$Cu(DMDCNQI)_2$	stack	8	1600	stack	130	1.3

TTM-TTP and τ-phase conductors

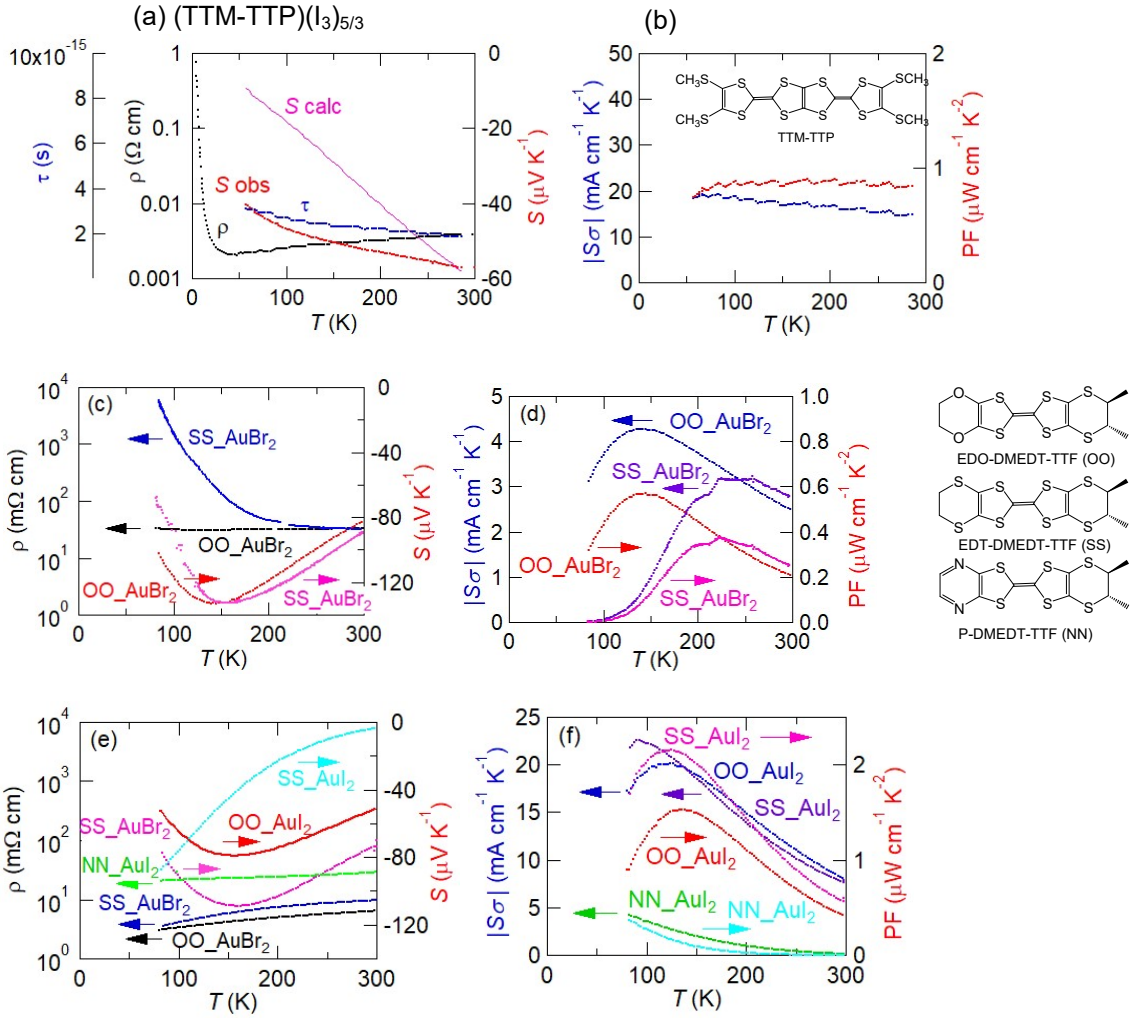

Fig. S2 (a) Resistivity, τ, and thermoelectric power, and (b) $S\sigma$ and PF of $(TTMTTP)(I_3)_{5/3}$. (c) Resistivity, τ, and thermoelectric power, and (d) $S\sigma$ and PF of τ-$(EDO\text{-}DMEDT\text{-}TTF)_2AuBr_2$ and τ-$(EDT\text{-}DMEDT\text{-}TTF)_2AuBr_2$. (e) Resistivity, τ, and thermoelectric power, and (f) $S\sigma$ and PF of τ-$(EDO\text{-}DMEDT\text{-}TTF)_2AuI_2$, τ-$(EDT\text{-}DMEDT\text{-}TTF)_2AuI_2$, and τ-$(P\text{-}DMEDT\text{-}TTF)_2AuI_2$. EDO-DMEDT-TTF: ethylenedioxy-*S*,*S*-dimethylethylenedithio-TTF EDT-DMEDT-TTF: ethylenedithio-*S*,*S*-dimethylethylenedithio-TTF, and P- DMEDT-TTF: pyrazino-*S*,*S*-dimethylethylenedithio-TTF.

BTBT and DMDCNQI

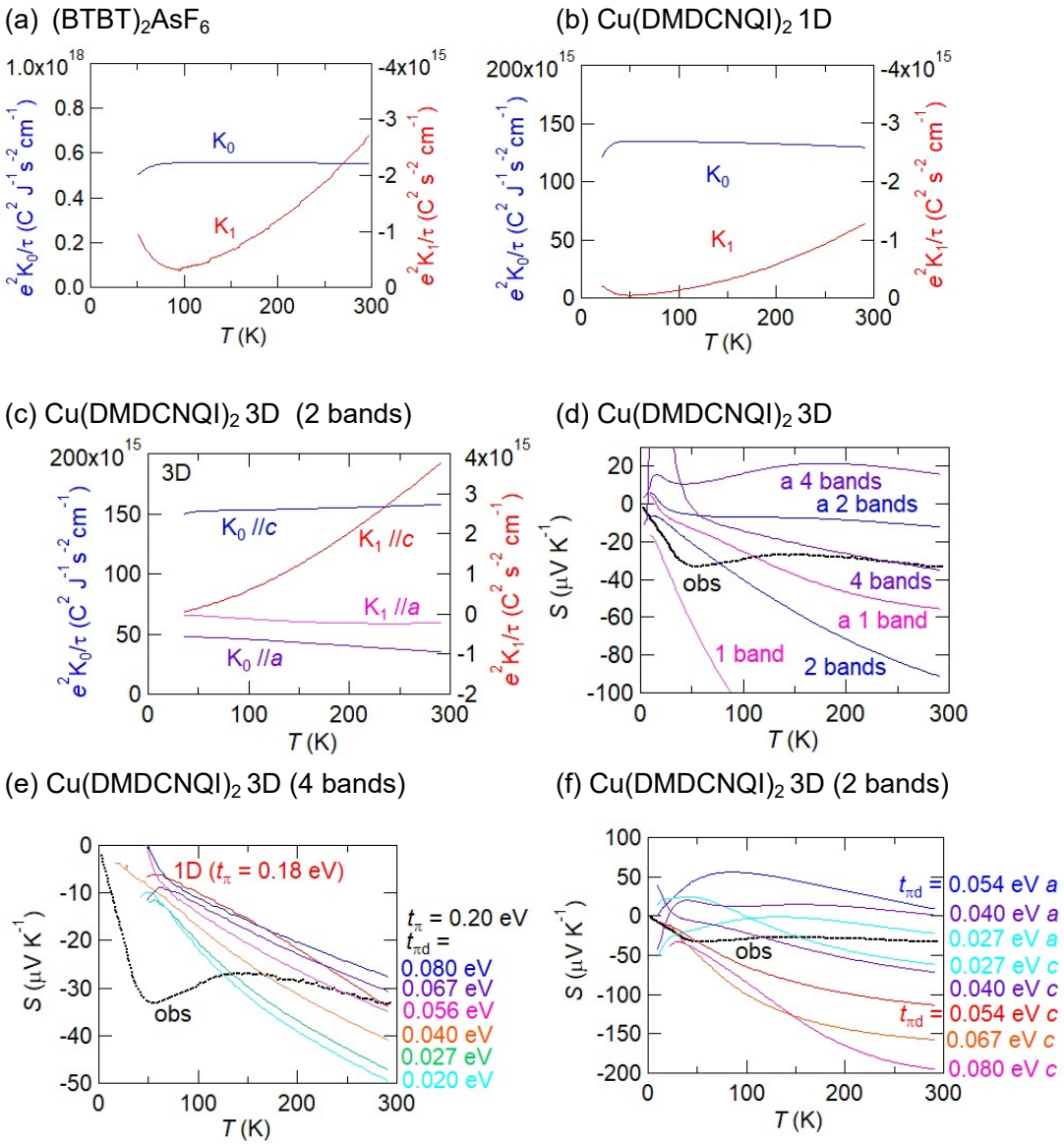

Fig. S3 Calculated K_0 and K_1 integrals of (a) $(BTBT)_2AsF_6$, (b) $Cu(DMDCNQI)_2$ based on the one-dimensional band, and (c) the three-dimensional two bands. (d) Calculated *S* along the *c* and *a* axes using the upper one, two, and four bands of $Cu(DMDCNQI)_2$ with t_c: 0.2, $t_{\pi d}$: 0.054, and Δ: 0.3 eV.[76] $t_{\pi d}$ dependence of *S* calculated for (e) upper four bands, and (f) two bands.

Due to the body centered symmetry, a unit of $Cu(DMDCNQI)_2$ contains four DMDCNQI molecules and two Cu atoms.[75] Considering the LUMO of DMDCNQI and a single 3d orbital of Cu, the energy bands consist of six bands (Fig. 7(e)). The resulting energy bands are identical to Ref. 77 using the same parameters, t_c: 0.2, $t_{\pi d}$: 0.054, and Δ: 0.3 eV.

Owing to the 3D character, the upper two bands afford large *S*, while *S* of the next two is small (Table S2). When all four bands are included, the resulting *S* is small (Fig. 7(f)) because *S* of a multiband is a weighted average of *S* with respect to K_0 following eqn (S3). Since the conductivity of a 1D band is larger than that of a 3D band (K_0 in Table S2), *S* is small even when a 3D band with large *S* participates in the conduction. Even increasing $t_{\pi d}$, the overall *S* decreases (Fig. S3(e)) because *S* of the 1D band decreases (Table S2). By contrast, *S* of the 3D band increases with increasing $t_{\pi d}$ (Fig. S3(f)). At the same time, *S* along the *a* axis shifts to the positive direction (Fig. S3(d) and (f)).

Even in the 3D band, *S* decreases with lowering the temperature. The observed increasing temperature dependence of *S* is not reproduced even including the Cu d orbital. The observed *S* is reproducible when the contribution of the 1D band is lost between 200 and 100 K potentially due to the 1D instability.

Table S2 *S*, K_0, and K_1 of each band in $Cu(DMDCNQI)_2$.

	S_c (rt) (μV K^{-1})			e^2K_0/τ (rt) ×10^{15} (C^2 J^{-1} s^{-2} cm^{-1})			e^2K_1/τ (rt) ×10^{15} (C^2 s^{-2} cm^{-1})		
$t_{\pi d}$ (eV)	0.27	0.54	0.80	0.27	0.54	0.80	0.27	0.54	0.80
1	−141	−156	−185	21	14	8.7	0.85	0.66	0.47
2	−100	−71	−56	33	37	38	0.97	0.75	0.62
3	−20	−13	−9	66	73	78	0.39	0.28	0.21
4	−20	−13	−9	66	73	78	0.39	0.28	0.21
sum	−47	−35	−28	186	198	202	2.6	1.97	1.51

References

S1 T. Mori, A. Kobayashi, Y. Sasaki, H. Kobayashi, G. Saito, H. Inokuchi, The intermolecular interaction of tetrathiafulvalene and bis(ethylenedithio)tetrathiafulvalene in organic metals. Calculation of orbital overlaps and models of energy-band structures, *Bull. Chem. Soc. Jpn*. 1984, **57**, 627.

S2 The software is available from http://indigo1026.la.coocan.jp/lib/program.html (accessed 1 July 2024).